Proceedings of the ASME 2010 3rd Joint US-European Fluids Engineering Summer Meeting and 8th International Conference on Nanochannels, Microchannels, and Minichannels
FEDSM-ICNMM2010
August 1-5, 2010, Montreal, Canada

FEDSM-ICNMM2010-30050

UNCERTAINTY QUANTIFICATION AND BIFURCATION BEHAVIOR OF AN AEROELASTIC SYSTEM

Ajit Desai
Department of Aerospace Engineering
Indian Institute of Technology Madras
Chennai, Tamil Nadu, 600036, India
Email: aerochajay44@gmail.com

Sunetra Sarkar*
Department of Aerospace Engineering
Indian Institute of Technology Madras
Chennai, Tamil Nadu, 600036, India
Email: sunetra.sarkar@gmail.com

ABSTRACT

Aeroelastic stability remains an important concern for the design of modern structures such as wind turbine rotors, more so with the use of increasingly flexible blades and military aircrafts with increasing maneuvering capabilities etc. A nonlinear aeroelastic system has been considered in the present study with parametric uncertainties. The analysis has been put in a stochastic framework and the propagation of system uncertainties have been quantified in the aeroelastic response. A spectral uncertainty quantification tool called Polynomial Chaos Expansion has been used. A projection based non-intrusive Polynomial Chaos approach is compared to its classical Galerkin based counterpart, and proven to be more efficient as order of chaos expansion increases. Effect of system randomness on the bifurcation behavior and the flutter boundary has been significant. Stochastic bifurcation results and bifurcation of probability density functions are presented here.

NOMENCLATURE

a_h Non-dimensional distance from airfoil mid-chord to elastic axis.
b Airfoil semi-chord.
C_L Lift coefficient.
C_M Pitching moment coefficient.
r_α Radius of gyration about elastic axis.
U Non-dimensional speed.
x_α Non-dimensional distance from elastic axis to center of mass.
α Pitch angle of airfoil.
ε Non-dimensional plunge displacement.
$\beta_\alpha, \beta_\varepsilon$ Cubic spring coefficients in pitch and plunge.
$\zeta_\alpha, \zeta_\varepsilon$ Viscus damping ratio in pitch and plunge.
μ Airfoil/air mass ratio.
τ Non-dimensional time.
ϖ Natural frequency ratio.

INTRODUCTION

Uncertainty quantification of aeroelastic systems is an important design concern for modern structures such as wind turbine rotors. With increasing flexibility of wind turbine blades [1] it has become even more crucial. Uncertainty in structural parameters, aerodynamic parameters and initial conditions etc, affects the characteristics of such dynamical systems. To make the computational aeroelastic model more trustworthy and reliable to predict aeroelastic stability, we put the problem into stochastic framework, which enables quantifying the propagation of system uncertainty into the response. The stochastic input has traditionally been analyzed with Monte Carlo simulation (MCS) [2]. However, it is computationally expensive as it needs a large number of realizations. Perturbation method is a fast tool for obtaining the response statistics in terms of its first and second order moments [3]. However, applications of this method are limited to small perturbation only and does not readily predict high or-

*Address all correspondence to this author, Tel.:+914422574024.

der statistics [4]. The resultant system of equations becomes extremely complicated beyond second order expansions as shown in the literature [5]. Sensitivity method is a more economical approach, based on the moments of samples, but it is less robust and depends strongly on modeling assumptions [6].

Polynomial chaos expansion (PCE) is a more effective approach pioneered by Ghanem and Spanos [5]. It uses a spectral representation of the system uncertainties in terms of orthogonal polynomials. Unlike perturbation method PCE allows high order statistics. The stochastic input is represented spectrally by employing orthogonal polynomials functionals from the generalized Askey scheme as basis in the random space [7]. The original homogeneous PCE was based on Hermite polynomials and it can give optimal exponential convergence for Gaussian inputs [8]. PCE based approaches have been examined extensively with different basis functions to model several uncertainty problems [9, 10].

A standard Galerkin projection is applied along the random dimension to obtain the weak form of the equation. The resultant deterministic systems are solved using standard time integration techniques to solve for each random mode [11]. Galerkin polynomial chaos expansion (Galerkin-PCE)(also called intrusive approach) modifies the governing equation to a coupled form in terms of the chaos coefficients. These are usually more complex and arriving at them are quite often a tedious task. In order to avoid these, several alternative approaches have been proposed. These are collectively called as non-intrusive methods. In non-intrusive PCE, samples of solutions of the differential equation are used to construct the coefficient of the polynomial chaos expansion. The probabilistic collocation method is such a non-intrusive method [12]. The non-intrusive polynomial chaos method proposed by Walter and co-workers [13–15] is based on approximating the polynomial chaos coefficients. A similar approach called non-intrusive spectral projection has been used by Reagan *et al.* [16]. Petit and Beran [17, 18] has also used this for an aeroelastic system.

In the subsequent sections, the intrusive and non-intrusive PCE approaches and their implementation with one and more random system parameters are discussed, and their combined effects on the bifurcation behavior of the aeroelastic system is studied in details.

NON-LINEAR AEROELASTIC SYSTEM

Figure 1 shows a schematic plot of the two degree-of-freedom pitch-plunge aeroelastic system and also the notations used in the analysis. The aeroelastic equations of motion for the linear system have been derived by Fung [19]. For nonlinear restoring forces such as with cubic springs in both pitch and plunge, the mathematical formulation is given by Lee *et al.* [20] in the non-dimensional form as follows:

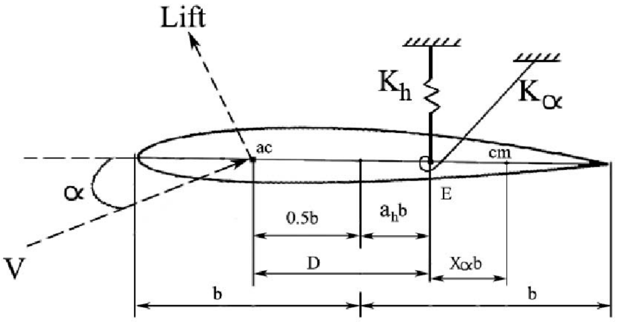

FIGURE 1. THE SCHEMATIC OF A SYMMETRIC AIRFOIL WITH PITCH AND PLUNGE DEGREES-OF-FREEDOM.

$$\varepsilon'' + x_\alpha \alpha'' + 2\zeta_\varepsilon \frac{\overline{\omega}}{U}\varepsilon' + \left(\frac{\overline{\omega}}{U}\right)^2(\varepsilon + \beta_\varepsilon \varepsilon^3) = -\frac{1}{\pi\mu}C_L(\tau)$$
$$\frac{x_a}{r_\alpha^2}\varepsilon'' + \alpha'' + 2\frac{\zeta_\alpha}{U}\alpha' + \frac{1}{U^2}(\alpha + \beta_\alpha \alpha^3) = \frac{2}{\pi\mu r_\alpha^2}C_M(\tau) \quad (1)$$

ζ_α and ζ_ε are the damping ratios in pitch and plunge respectively, β_α and β_ε denotes coefficients of cubic spring in pitch and plunge respectively. For incompressible, in-viscid flow, Fung [19] gives the expressions for unsteady lift and pitching moment coefficients, $C_L(\tau)$ and $C_M(\tau)$.

Using Wagner function and introducing the following new variables w_1, w_2, w_3, w_4, the original integro-differential equations for aeroelastic system given by Eqn. (1) are reformulated into set of first order autonomous differential equations,

$$x' = f(\boldsymbol{X}, \text{ system parameters}) \quad (2)$$

where $\boldsymbol{X}$ is an array of eight variables as given below; $\{x_1, x_2, x_3, x_4, x_5, x_6, x_7, x_8\} = \{\alpha, \alpha', \varepsilon, \varepsilon', w_1, w_2, w_3, w_4\}$. For detail, refer to Lee *et al.* [20],

UNCERTAINTY QUANTIFICATION AND POLYNOMIAL CHAOS EXPANSION

It is increasingly being felt among the aeroelastic community that aeroelastic analysis should include the effect of parametric uncertainties. This can potentially revolutionize the present design concepts with higher rated performance and can also reshape the certification criteria. Nonlinear dynamical systems are known to be sensitive to physical uncertainties, since they often amplify the random variability with time. Hence, quantifying the effect of uncertainty propagation on the aeroelastic stability boundary is crucial. Flutter, a dynamic aeroelastic instability involves a Hopf bifurcation where a damped (stable response) oscillation changes to a periodic oscillatory response at a critical wind velocity. In a linear system this post flutter response can grow in an unbounded fashion [19]. System parametric uncertainties can significantly affect the onset and properties of bifurcation points. The importance of stochastic modeling of these uncertainties is that they can quantify the effect of the uncertainties on flutter and bifurcation in a probabilistic sense and gives the response statistics in a systematic manner.

The original homogeneous polynomial chaos expansion [5] is based on the homogeneous chaos theory of Wiener [21, 22]. This is based on a spectral representation of the uncertainty in terms of orthogonal polynomials. In its original form, it employs Hermite polynomials as basis from the Askey scheme in terms of Gaussian random variables [22]. According to Cameron-Martin theorem [23], it can approximate any functionals in $L_2(C)$ and

converges in the $L_2(C)$ sense, where C is the space of real functions which are continuous on the interval [0,1] and vanish at 0. Therefore, polynomial chaos provides a means for expanding second-order random processes in terms of Hermite polynomials. Second order random processes are processes with finite variance, and this applies to most physical processes [11].

Spectral polynomial chaos based approaches with other basis functions have also been used in the recent past in various unsteady flow and flow-structure interaction problems of practical interest [24, 25].

Polynomial Chaos Expansion

As per the Cameron-Martin theorem [23], a random process $X(t,\theta)$, viewed as function random event θ, which is second order stationary can be written as,

$$X(t,\theta) = \widehat{a}_0\psi_0 + \sum_{i_1=1}^{\infty} \widehat{a}_{i_1}\psi_1(\xi_{i_1}(\theta)) + \sum_{i_1=1}^{\infty}\sum_{i_2=1}^{i_1} \widehat{a}_{i_1 i_2}\psi_2(\xi_{i_1}(\theta),\xi_{i_2}(\theta)) + \sum_{i_1=1}^{\infty}\sum_{i_2=1}^{i_1}\sum_{i_3=1}^{i_2} (\widehat{a}_{i_1 i_2 i_3})\psi_3(\xi_{i_1}(\theta),\xi_{i_2}(\theta),\xi_{i_3}(\theta)) + \ldots, \quad (3)$$

where, $\psi_n(\xi_{i_1},\ \xi_{i_2},\ldots\ldots\xi_{i_n})$ denotes the Hermite polynomial of order n in terms of n-dimensional independent standard Gaussian random variables $\boldsymbol{\xi} = (\ \xi_{i_1},\xi_{i_2},\ldots\ldots\xi_{i_n})$ with zero mean and unit variance. The above equation is the discrete version of the original Wiener polynomial chaos expansion, where the continuous integrals are replaced by summations. For notational convenience Eqn. (3) can be rewritten as:

$$X(t,\theta) = \sum_{j=0}^{\infty} a_j \Phi_j(\boldsymbol{\xi}(\theta)) \quad (4)$$

There is an one-to-one relationship between the ψ's and Φ's and also $\widehat{a}_j$'s and a_j's in Eqn. (3) and Eqn. (4). In the original form, ψ_ns were Hermite polynomials. The first few one-dimensional Hermite polynomials are given as:

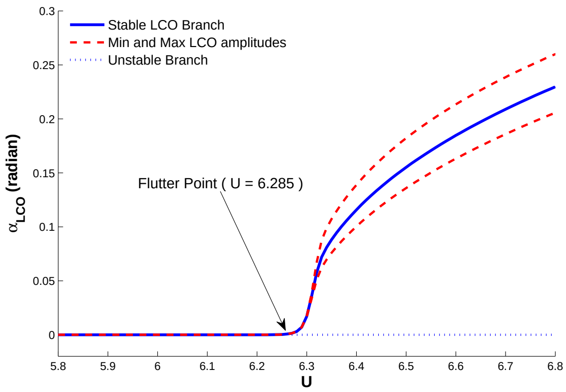

FIGURE 2. UNCERTAIN CUBIC SPRING: STOCHASTIC BIFURCATION DIAGRAM (SUPERCRITICAL Hopf BIFURCATION).

$$\begin{aligned}
\psi_0 &= 1, \\
\psi_1 &= \xi, \\
\psi_2 &= \xi^2 - 1, \\
\psi_3 &= \xi^3 - 3\xi, \\
\psi_4 &= \xi^4 - 6\xi^2 + 3,
\end{aligned}$$

Other Hermite polynomials can be generated from the following recurrence relationship,

$$\psi_n = \xi\psi_{n-1} - (n-1)\psi_{n-2}.$$

However, the exponential convergence of the polynomial chaos expansion has been extended to several other types of commonly used probability distributions. One can use orthogonal polynomials from the generalized Askey scheme for some standard non-Gaussian input uncertainty distributions such as gamma and beta [24]. For any arbitrary input distribution, a Gram-Schmidt orthogonalization can be employed to generate the orthogonal family of polynomials [26]. Any stochastic process $\alpha(t,\boldsymbol{\xi}(\theta))$, governed by Gaussian random variable ξ (ξ can always be normalized as a standard Gaussian one) can then be approximated by the following truncated series:

$$\alpha(t,\theta) = \sum_{j=0}^{p} \hat{\alpha}_j(\mathrm{t})\ \Phi_j(\boldsymbol{\xi}(\theta)) \quad (5)$$

Note that, here the infinite upper limit of Eqn. (4) is replaced by p, called the order of the expansion. For multi-dimensional

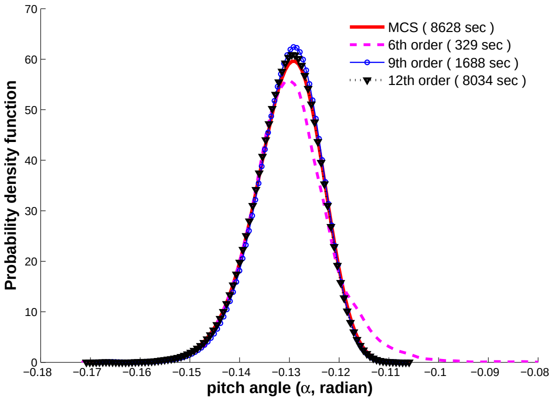

FIGURE 3. UNCERTAIN CUBIC SPRING: PDF COMPARISON WITH INCREASING ORDER OF GALERKIN-PC EXPANSION, WITH $U = 6.42$.

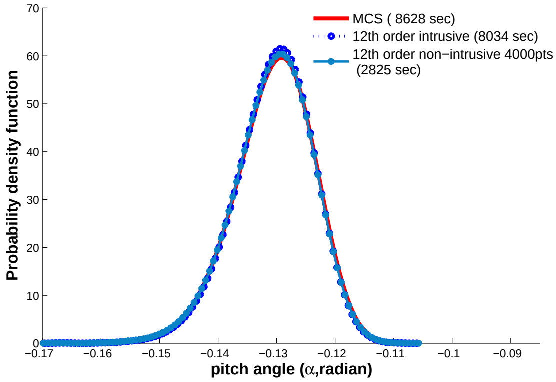

FIGURE 4. UNCERTAIN CUBIC SPRING: PDF COMPARISON FOR INTRUSIVE AND NON-INTRUSIVE PCE, WITH $U = 6.42$

random variables (n), with number of polynomial terms denoted by n_p, it is given by the following [7].

$$p = \frac{(n+n_p)!}{n!n_p!} - 1 \tag{6}$$

Classical Galerkin Polynomial Chaos Approach In the classical Galerkin-PCE approach, the polynomial chaos expansion of the system response is substituted into the governing equation and a Galerkin error minimization in the probability space is followed. This results in a set of coupled equations in terms of the polynomial chaos coefficients. The resulting system is deterministic, but they are significantly modified to a higher order and complexity depending on the order of chaos expansion and system nonlinearity. After solving this set of coefficient equations, they are substituted back to get the system response.

We demonstrate the Galerkin-PCE approach for a generalized dynamical system for a single random variable case, that is, with a random cubic stiffness. Let us write the governing equation with a cubic nonlinearity in the following form [25],

$$\pounds[\alpha(t,\theta)] + \beta_\alpha[\alpha(t,\theta)]^3 = 0, \tag{7}$$

here, $\pounds$ is a linear differential operator. If the cubic spring stiffness is assumed to be a Gaussian random variable with mean $\bar{\beta}_\alpha$ and standard deviation $\widetilde{\beta_\alpha}$, it can be characterized by,

$$\beta_\alpha = \bar{\beta}_\alpha + \xi\widetilde{\beta}_\alpha \tag{8}$$

Substituting the chaos expansion terms in Eqn. (7), and using a Galerkin projection $< ., \ \phi_k >$, for $k = 0, 1, ...p$, and simplifying we get;

$$\pounds[\widehat{\alpha}_k] + \frac{1}{<{\Phi_k}^2>} \sum_{l=0}^{1}\sum_{i=0}^{p}\sum_{m=0}^{p}\sum_{n=0}^{p} \beta_{\alpha l}\ \widehat{\alpha}_i\ \widehat{\alpha}_m\ \widehat{\alpha}_n < \Phi_l\ \Phi_i\Phi_m\Phi_n\Phi_k >= 0 \tag{9}$$

Here, $\beta_{\alpha 0} = \bar{\beta}_\alpha$ and $\beta_{\alpha 1} = \widetilde{\beta}_\alpha$. The expected value operator,$< >$, called the inner product is defined as,

$$< \Phi_l...\Phi_k > \ = \int_{-\infty}^{\infty} \Phi_l...\Phi_k\ \omega(\xi)\ \mathrm{d}\xi. \tag{10}$$

Where the weighting function $\omega(\xi)$, is the Gaussian probability density function. For single random variable case it is given as:

$$\omega(\xi) = (\frac{1}{\sqrt{2\pi}})\ e^{-(\frac{1}{2}\ \xi^2)}, \tag{11}$$

The Galerkin approach is also called the intrusive approach as it modifies the system governing equation in terms of the chaos coefficients. The modification results into a higher order and much more complex form of the equations. As a result, this approach may become computationally quite expensive as order of expansion increases [18, 27].

Non-intrusive Projection Method A number of non-intrusive variants of PCE have been developed to counter the disadvantages of the classical Galerkin method. Stochastic projection is one of them [5, 28]. In the present study, a stochastic projection based approach is used to evaluate the chaos coefficients. Here, the chaos expansions are not substituted in the governing

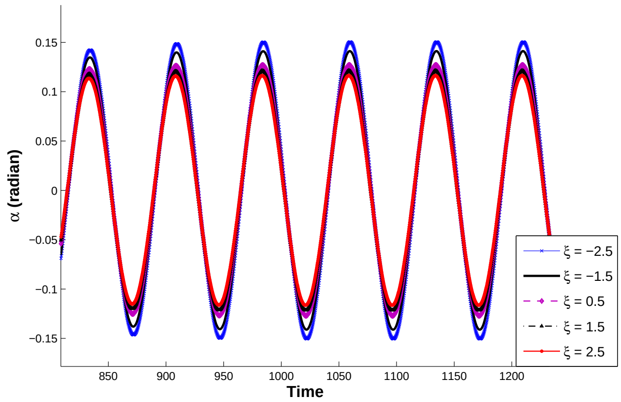

FIGURE 5. UNCERTAIN CUBIC SPRING: FIVE DIFFERENT REALIZATION TIME HISTORIES AT $U = 6.42$.

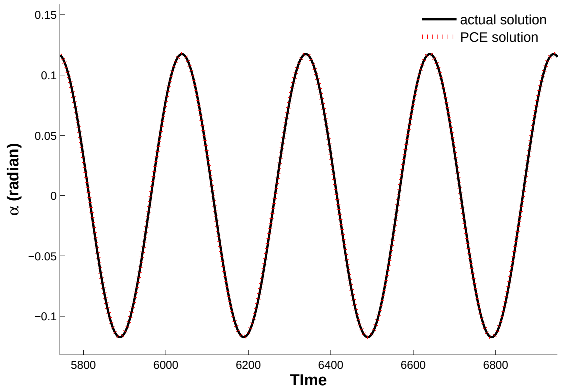

FIGURE 6. UNCERTAIN CUBIC SPRING: A TYPICAL TIME HISTORY WITH 12$^{\text{th}}$ ORDER PCE AND MCS FOR $\xi = 1.5$ AND $U = 6.42$.

equations; instead samples of the solutions are used (using a low order pseudo-Monte Carlo method) to evaluate the coefficients directly using a projection formula. As a result, this approach can utilize the existing deterministic code and hence the name non-intrusive. The random process is approximated by a truncated series, as shown in Eqn. (5).

The Hermite polynomials are statistically orthogonal, that is, they satisfy $<\Psi_i, \Psi_j>= 0$ for $i \neq j$, hence the expansion coefficients can be directly evaluated as:

$$\widehat{\alpha}_j(t) = \frac{<\alpha(t,\theta), \Phi_j>}{<{\Phi_j}^2>} \tag{12}$$

The denominator in Eqn. (12) can be shown to satisfy $<{\Phi_j}^2> = j\,!$ for non-normalized Hermite polynomials [17].

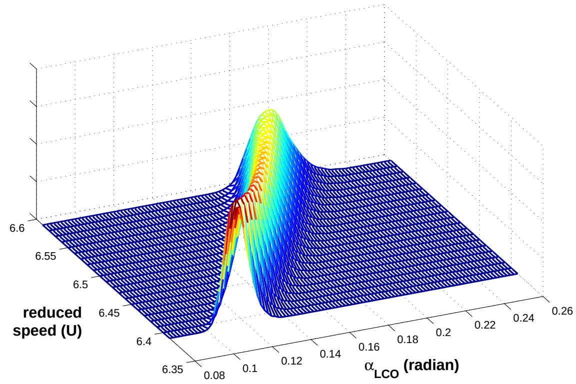

FIGURE 7. UNCERTAIN CUBIC SPRING: AMPLITUDE RESPONSE PDF AS A FUNCTION OF REDUCED SPEED.

So the key step in projecting $\alpha(t,\theta)$ along the polynomial chaos basis is the evaluation of $<\alpha, \Phi_j>$. This is done by a numerical integration scheme using Simpson's rule by employing Eqn. (13).

For two random variable, (ξ_1 and ξ_2).

$$<\alpha(t,\theta), \Phi_k> = \int_{-\infty}^{\infty}\int_{-\infty}^{\infty} \alpha(t,\theta)\ \Phi_k\ \omega(\boldsymbol{\xi})\ \mathrm{d}\xi_1 \mathrm{d}\xi_2. \tag{13}$$

Where the weighting function $\omega(\boldsymbol{\xi})$ is the Gaussian probability density function is given by the following,

$$\omega(\boldsymbol{\xi}) = (\frac{1}{\sqrt{(2\pi)^2}})\ e^{-\frac{1}{2}\ ({\xi_1}^2+{\xi_2}^2)} \tag{14}$$

A pseudo Monte Carlo Simulation approach employing N samples of ξ_1 and ξ_2 is used (N being lesser than that used in a full MCS) to generate the response realizations. The samples of ξ_1 and ξ_2 are taken as the equi-probability points (for the definition of equi-probability points, see [29]). The corresponding β_α and ζ_α samples (from Eqn. (8)) are used to run the pseudo-MCS. The realizations of the system response $\alpha(t,\theta)$ are then used to estimate the deterministic coefficients, $\widehat{\alpha}_j(t)$s in Eqn. (12) using the Simpson's rule. More efficient approaches that could be considered for practical implementation include the many efficient sampling techniques [30], which should improve the convergence of the MCS, and Gauss-Hermite quadrature of the integral. However, the results presented below show that oscillatory random process become increasingly oscillatory in the random dimension as time progresses, which suggest that even Gauss quadrature would require many samples to yield acceptable accuracy also suggested by Pettit and Beran [17].

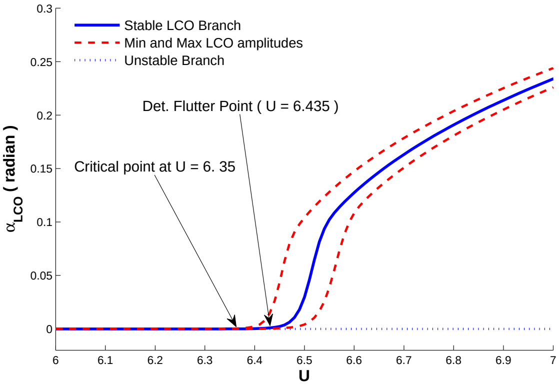

FIGURE 8. UNCERTAIN VISCOUS DAMPING: STOCHASTIC BIFURCATION PLOT.

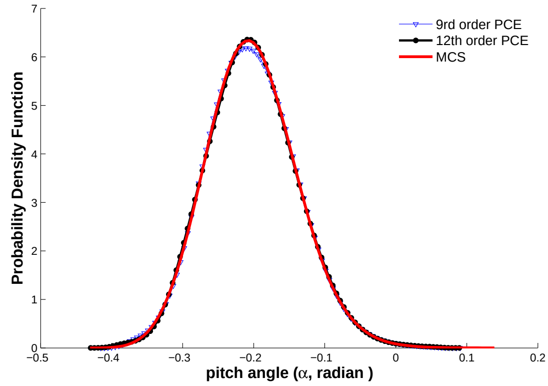

FIGURE 10. UNCERTAIN VISCOUS DAMPING: COMPARISON OF THE PDFs WITH INCREASING ORDER OF PCE AT NONDIMENSIONAL TIME $t = 1400$ AND $U = 6.52$.

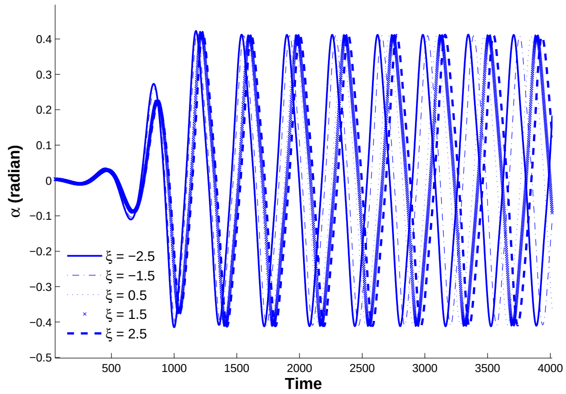

FIGURE 9. UNCERTAIN VISCOUS DAMPING: FIVE DIFFERENT REALIZATION TIME HISTORIES AT $U = 6.52$.

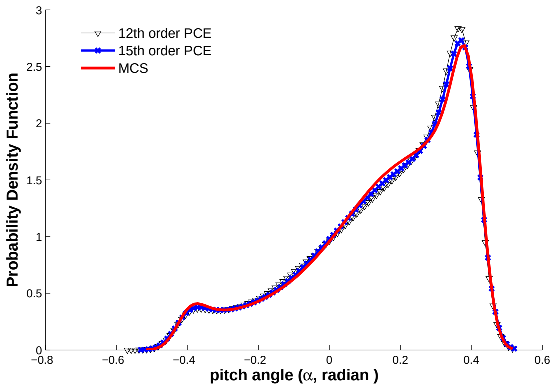

FIGURE 11. UNCERTAIN VISCOUS DAMPING: COMPARISON OF THE PDFs WITH INCREASING ORDER OF PCE AT NONDIMENSIONAL TIME $t = 5000$ AND $U = 6.52$.

RESULTS AND DISCUSSION

The main focus of the present study is quantifying the effects of parametric uncertainty of the system on the bifurcation behavior and the flutter boundary. In this paper we will consider a single random variable model first, then a two random variable case.

The parameter values used for calculation are [20]: $\mu = 100, \bar{\omega} = 0.2, a_h = -0.5, \ x_\alpha = 0.25, \zeta_\alpha = 0, \zeta_\varepsilon = 0, \ r_\alpha = 0.5, \ \beta_\alpha = 3, \ \beta_\varepsilon = 0$. First, consider a single random variable model, the cubic hardening spring is assumed to be a Gaussian random variable with mean $\bar{\beta}_\alpha$ =3 and standard deviation $\widetilde{\beta}_\alpha$ =0.3. Fig. 2 shows bifurcation behavior for the supercritical response, with the cubic stiffness as random, it now has a range of possible LCO amplitudes for each reduced velocities and the onset of flutter is unaffected. The standard deviation, that is, the amplitude variation range increases as reduced speed increases. These results are obtained by using MCS.

A Galerkin-PCE approach is used to quantify the propagation of this uncertainty on the response. The Galerkin approach modifies the 8^{th} order system to a $8 \times (p+1)$ order system. It also involves calculating the complex fifth order inner product terms, as shown in Eqn. (9), which are calculated before-hand by using symbolic mathematical solver *Mathematica* and used in the solution. As a result, the solution process is computationally intensive for the nonlinear system in question. After solving for the chaos coefficients, in the post processing stage, the coefficients are substituted back to the expansion form to get the stochastic response. Probability density functions (PDFs) and other required statistics can then be readily obtained. Fig. 3 shows, a representative PDF for increasing order of chaos expansion at a time instant when the solutions are well past their transients and is sta-

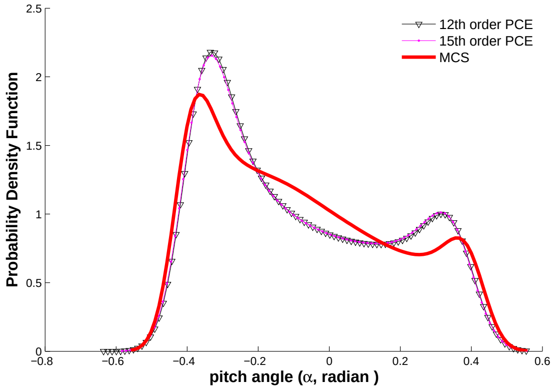

FIGURE 12. UNCERTAIN VISCOUS DAMPING: COMPARISON OF THE PDFs WITH INCREASING ORDER OF PCE AT NONDIMENSIONAL TIME $t = 7800$ AND $U = 6.52$.

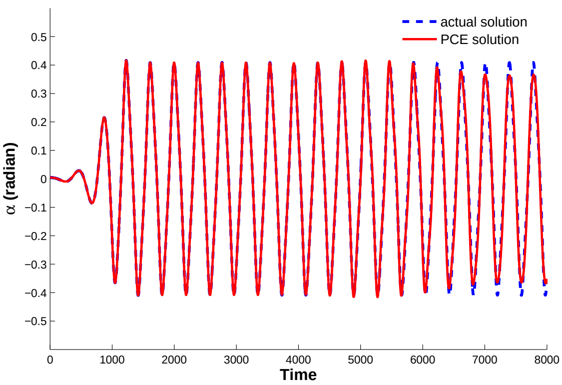

FIGURE 13. UNCERTAIN VISCOUS DAMPING: A TYPICAL TIME HISTORY WITH 15$^{\text{th}}$ ORDER PCE AND MCS AT $\xi = 2.3$ AND $U = 6.52$.

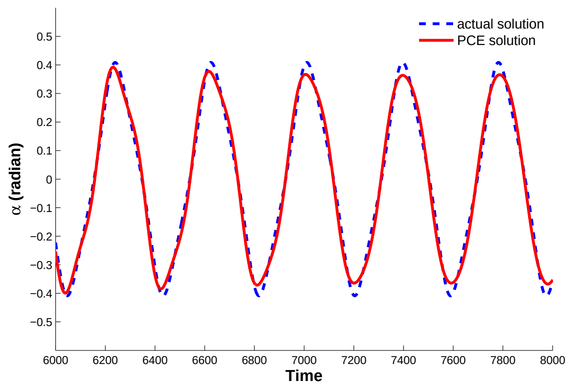

FIGURE 14. UNCERTAIN VISCOUS DAMPING: BLOWN UP VERSION OF THE SAME TIME HISTORY GIVEN IN FIG. 13

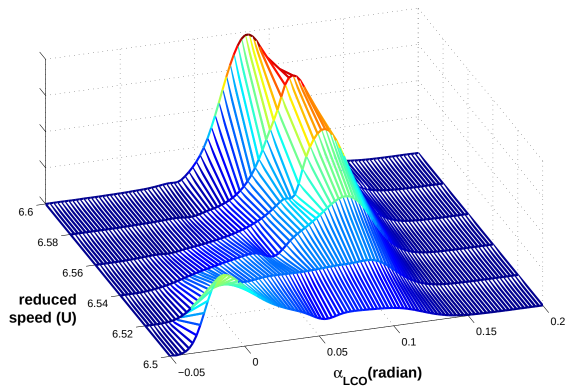

FIGURE 15. UNCERTAIN VISCOUS DAMPING: AMPLITUDE RESPONSE PDF AS A FUNCTION OF REDUCED SPEED.

tionary. The reduced speed is considered to be $U = 6.42$, close to the deterministic bifurcation point. The figure shows how increasing the order of expansion the CPU time for the solve is increasing. For the 12$^{\text{th}}$ order expansion the CPU time is almost same as MCS and PDF is matching well with that of MCS. Thus the computational disadvantages of the conventional Galerkin-PCE for nonlinear system is easily demonstrated.

A more effective way to evaluate the chaos coefficients without solving coupled differential equation is the projection method. With the projection approach, for the same random variation of the uncertain cubic spring stiffness, the PDF is calculated and compared with that of Galerkin-PCE in Fig. 4. Both match well but projection approach takes comparatively less CPU time. We used a 12000 sample standard MCS results as reference solution. The pseudo-MCS needed to estimate the chaos coefficients with the projection approach is of much lower order. The sampling points chosen for this are the equi-probability points in the random domain, with the range from -4 to 4 [29]. Projection based non-intrusive PCE method is proved to be computationally much-more efficient than the conventional Galerkin based PCE and hence, in the remaining part of the paper we will use non-intrusive PCE method.

The response realization time histories for a few samples of random variable are plotted in Fig. 5, The response time histories show difference in amplitude but not in phase. A typical realization time history obtained with PCE along with its deterministic counterpart is given in Fig. 6, in a blown up version. The match is perfect even at long time. Amplitude response PDFs as a function of reduced velocities (bifurcation parameter) are shown in Fig. 7. They represent single peak monotonic behavior as all the realizations give finite amplitude LCOs. Effectively, the PDFs are not undergoing any bifurcations. Close to U=6.4 the PDF

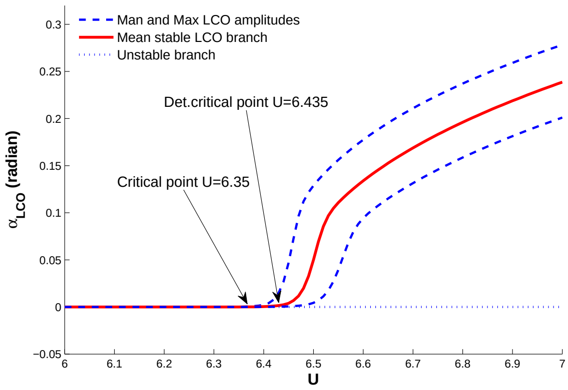

FIGURE 16. UNCERTAIN β_α AND ζ_α: STOCHASTIC BIFURCATION PLOT.

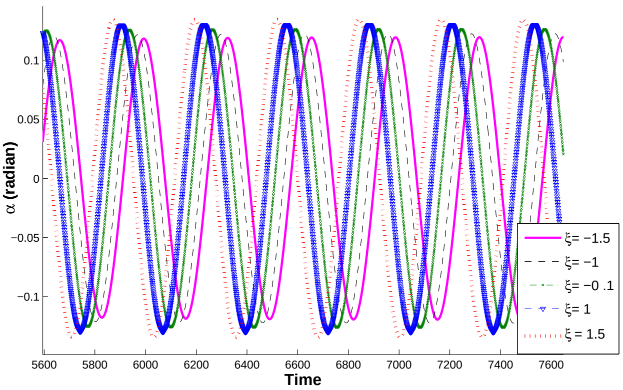

FIGURE 17. UNCERTAIN β_α AND ζ_α: BLOWN UP VERSION OF THE FIVE DIFFERENT REALIZATION TIME HISTORY AT $U = 6.52$.

looks sharper and narrower as most realizations are going towards the same limit cycle amplitude. As the speed increases, the PDF is broader and less sharp, indicating that the realization amplitudes are spread over a wider band of amplitudes.

Next, we consider the viscous damping ratio in pitch (ζ_α) to be uncertain (in the earlier part damping was put to be zero) and all the other parameters deterministic. This case seems more interesting than the earlier one. The damping ratio is assumed to be a Gaussian random variable with mean $\bar{\zeta}_\alpha$ =0.1 and standard deviation $\tilde{\zeta}_\alpha$ =0.01. Fig. 8 shows the bifurcation behavior with random damping ration. Now, the stochastic onset of flutter is well below the deterministic onset, we now have the range of flutter points.

In this case, the response realizations are shifted in phase from each other due to random damping ratios. This becomes

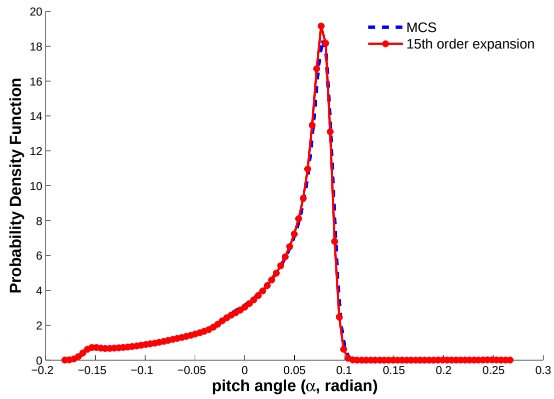

FIGURE 18. UNCERTAIN β_α AND ζ_α: COMPARISON OF THE PDFs OBTAINED BY PCE AND MCS AT NONDIMENSIONAL TIME $t = 4000$ AND $U = 6.52$.

more pronounced with time as shown in Fig. 9. Five different realizations time histories have been presented here for different values of the random variable ζ_α. The response PDF at non-dimensional time 1400 and $U = 6.52$ is shown in Fig. 10. A reasonably good match with MCS results is observed for a 12$^{\text{th}}$ order expansion. Please note that this time level is past the initial transients. Due to the phase shifting time histories of the response realizations, the PDF at higher time levels take a deformed shape from the monotonic single peak behavior. Fig. 11 shows the PDF at non-dimensional time 5000 and $U = 6.52$, in which a double-peak bimodal PDF is emerging. In this case a 12$^{\text{th}}$ order expansion is not sufficient to capture the response accurately, a 15$^{\text{th}}$ order expansion gives better results. At non-dimensional time 7800 with same reduced speed, the response PDF is more deformed and gives a two-peak bimodal shape more clearly as seen in Fig. 12. However, even a 15$^{\text{th}}$ order chaos expansion does not give the required accuracy. The reason for the mismatch is apparent from Fig. 13. A typical realization time history with PCE along with its deterministic counterpart is presented. A blown up version of the same plot is given in Fig. 14. One can clearly see a degeneracy in the time history, which starts near time levels close to 6000. PCE can show such type of degenerate behavior in capturing LCO response [18], especially at very large times. This is known as large time degeneracy. As a counter measure, one can increase the order of the chaos expansion. However, this can only push the degeneracy to a later time and can not solve it entirely. Non-polynomial based chaos expansion approaches have also been attempted in the recent past towards this end [18]. An unsteady adaptive stochastic finite elements method, developed by Witteveen and Bijl [31–33] has been used successfully. In this method interpolation of oscillatory samples is based on constant phase instead of a constant time.

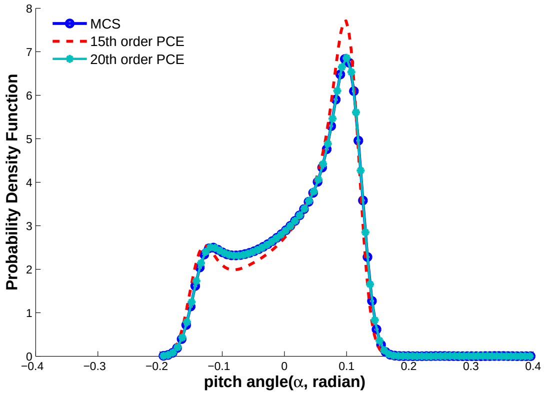

FIGURE 19. UNCERTAIN β_α AND ζ_α: COMPARISON OF THE PDFs OBTAINED BY PCE AND MCS AT NONDIMENSIONAL TIME $t = 5000$ AND $U = 6.52$.

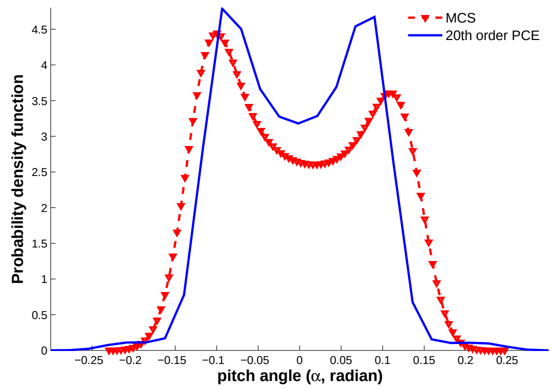

FIGURE 20. UNCERTAIN β_α AND ζ_α: COMPARISON OF THE PDFs OBTAINED BY PCE AND MCS AT NONDIMENSIONAL TIME $t = 7800$ AND $U = 6.52$.

Amplitude response PDFs as a function of reduced speed are shown in Fig. 15. A non-monotonic behavior is clearly indicated; some realizations are going to damped oscillation and others give LCO amplitudes scattered within the domain boundary. At $U = 6.5$, the double-peak behavior of the PDF indicates the two different LCO amplitudes around which most of the realizations are concentrated. Towards $U = 6.6$, all realizations give finite amplitude LCO, thus essentially they are of the same type. The PDF shows a single-peak monotonous behavior. Therefore, the PDFs of the response amplitude have clearly gone through a qualitative change here, in other words, a bifurcation. This shows that the dynamics of this nonlinear aeroelastic system is very sensitive to system uncertainty in this range of reduced velocities. The PDFs also clearly show the probability of entering into LCO (i.e. flutter) which highlights the risk induced by uncertain parametric variation.

Next, we consider the two random variable case. Parametric uncertainty is modeled in cubic spring coefficient, β_α and viscus damping ratio, ζ_α. These parameters are assumed to be Gaussian random variable with mean values of 3.0 and 0.1 respectively; each assumed to have the coefficient of variation of 0.10. They are assumed to be independent random variables. The bifurcation plots in Fig. 16 shows, the combined effects of first two cases (see Fig. 2 and Fig. 8), that is, onset of flutter changes, and also amplitude variation range increases as reduced speed increases. Fig. 17 shows the time histories for five different realizations, the response realizations are shifted in phase and also their amplitude varies from each other, this is due to uncertainties in both β_α and ζ_α. This becomes more pronounced as time precedes.

The response PDF at $U = 6.52$ and non-dimensional time 4000 is shown in Fig. 18. A reasonably good match with MCS results is observed for a 15^{th} order expansion. Please note that at this time level most of the response realizations are past the initial transients, though not all. Due to large phase shifting, each of the time history takes different time interval to enter into LCO. And the PDF at higher time levels take a deformed shape from a single peak behavior. Fig. 19 shows the PDF at non-dimensional time 5000 in which a double-peak bimodal behavior is emerging. In this case a 15^{th} order expansion has not been sufficient to capture the response accurately. A 20^{th} order expansion gives better results. At non-dimensional time 7800, the response PDF is more deformed and gives a two-peak bimodal shape more clearly as seen in Fig. 20. However, even a 20^{th} order chaos expansion does not give the required accuracy. The reason for the mismatch is apparent in Fig. 21. A typical realization time history with PCE along with its deterministic counterpart in blown up version is given. One can clearly see how the time history gives a perfect match at earlier times but fails at large times that is large

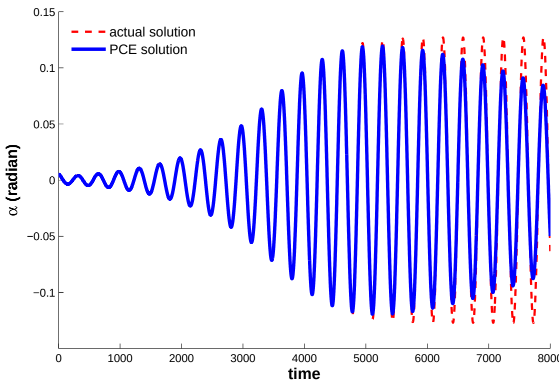

FIGURE 21. UNCERTAIN β_α AND ζ_α: A TYPICAL TIME HISTORY WITH 15^{th} ORDER PCE AND MCS AT $\xi = 1.5$ AND $U = 6.52$.

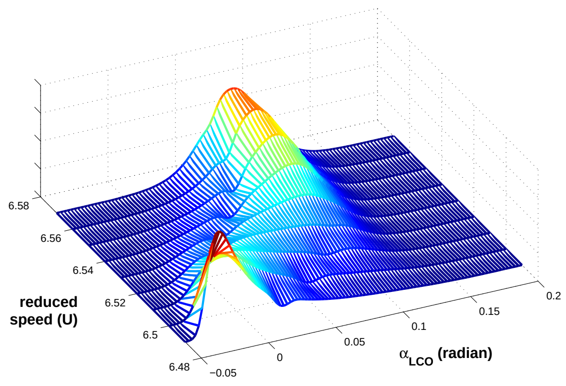

FIGURE 22. UNCERTAIN β_α AND ζ_α: AMPLITUDE RESPONSE PDF AS A FUNCTION OF REDUCED SPEED.

degeneracy in the time history. Here, PCE is unable to capture the behavior at long time. As discussed earlier one can increase the order of chaos expansion (more than 20^{th} order expansion). However, this only push degeneracy to a later time but can not solve it entirely. Galerkin-PCE with higher order expansion will also give the same results. However, due to excessively high computational cost this simulation is not included in the paper.

Figure 22 shows the amplitude response PDFs as a function of the reduced speed. At $U = 6.49$ as the bimodal behavior of the PDF indicates, most of the realizations are concentrated towards $\alpha = 0$ and only few go to some positive value of α. At $U = 6.52$ PDF is almost flat, all realizations are distributed between $\alpha = 0$ and some positive value. At $U = 6.55$, the PDF is again bimodal but more realizations are concentrated towards some positive values of α and only few towards $\alpha = 0$. At any U above 6.56 PDFs have single-peak monotonous behavior. Therefore, the PDFs of the response amplitude have clearly gone through a qualitative change. These changes are more prominent in two random variable case compared to the single variable random damping case as was shown in Fig. 15.

CONCLUSIONS

The bifurcation behavior of a nonlinear pitch-plunge flutter problem with uncertain system parameters has been studied. The problem is a simple model problem to understand the mechanism of nonlinear flutter in a stochastic framework. The parametric randomness could be attributed to the uncertainties encountered during laboratory dynamical experiments. A cubic nonlinear stiffness could represent various sources of analytic nonlinearities; they often represent different control mechanisms.

The Galerkin polynomial chaos method and the projection method are applied to propagate the uncertainties through the system. The focus of this work is to investigate the performance of these techniques and to see how the aeroelastic stability characteristics are altered due to the random effects. The results of both the methods are compared to a reference Monte Carlo solution. The computational cost of the Galerkin polynomial chaos method was prohibitively high as order of expansion increases, hence, for large order expansion the projection method can be used to save CPU time. The effect of uncertain cubic structural nonlinearity and viscous damping parameter are investigated separately as well as simultaneously. Uncertainty in the cubic stiffness has not altered the deterministic bifurcation (flutter) point, it only affects the amplitudes of the periodic response in the post flutter stage. The PDF behavior also does not show any qualitative changes. On the other hand, uncertainty in damping changes the bifurcation point. It can lower the onset of flutter which seems to be more dangerous. The PDF of the response amplitude also undergoes a qualitative change. When both cubic spring stiffness and viscous damping ratio are taken randomly, the effects on bifurcation behavior of the system are more prominent. The amplitude as well as onset of flutter varies. The PDF response amplitude undergoes qualitative changes. In other words, bifurcation of the response PDF takes place which clearly shows the risk induced by parametric uncertainty and importance of uncertainty quantification. Thus the effects on the bifurcation and stability of the nonlinear aeroelastic systems are more prominent when uncertain system parameters are taken together rather than as single.

REFERENCES

[1] Tanver, P., 2008. "Wind power as a clean-energy contributor". *Energy Policy,* ***36***, pp. 4397–4400.

[2] Pettit, C. L., and Beran, P. S., 2003. "Effects of parametric uncertainty on aifroil limit cycle oscillation". *J. Aircraft,* ***40***, pp. 1004–1006.

[3] Kleiber, M., and Hien, T. D., 1992. *The Stochastic Finite Element Method: Basic Perturbation Technique and Conmputer Implementation*. John Wiley and Sons, New York.

[4] Ghosh, R., Chakraborty, S., and Bhattacharyya, 2001. "Stochastic sensitivity analysis of structures using first order perturbation". *Mechanics.,* ***36***, pp. 291–296.

[5] Ghanem, R. G., and Spanos, P., 1991. *Stochastic Finite Elements: a Spectral Approach*. Springer-Verlag, New York.

[6] Hills, R. G., and Trucano, T. G., 1999. Statistical validation of engineering and scientific models: background, May. URL http://citeseerx.ist.psu.edu/viewdoc/summary?doi=10.1.1.40.1901.

[7] Xiu, D., and Karniadakis, G. E., 2002. "The Wiener-Askey polynomial chaos for stochastic differential equations". *SIAM Journal on Scientific Computing,* ***24***(2), pp. 619–644.

[8] Ghanem, R., 1999. "Stochastic finite elements with mul-

tiple random non-Gaussian properties". *Journal of Engineering Mechanics,* ***125***, pp. 26–40.

[9] Karniadakis, G. E., and Lucor, D., 2004. "Predictability and uncertainty in flow-structures interactions". *European Journal of Mechanics B/Fluids,* ***23***, pp. 41–49.

[10] Lin, G., Su, C. H., and Karniadakis, G. E., 2006. "Predicting shock dynamics in the presence of uncertainties". *Journal of Computational Physics,* ***217***, pp. 260–276.

[11] Xiu, D., and Karniadakis, G. E., 2003. "Modeling uncertainty in flow simulations via generalized polynomial chaos". *Journal of Computational Physics,* ***187***, pp. 137–167.

[12] Loeven, G., Witteveen, J. A. S., and Bijl, H., 2007. "Probabilistic collocation: an efficient non-intrusive approach for arbitrarily distributed parametric uncertainties". 45$^{\text{th}}$ *AIAA Aerospace Sciences Meeting and Exhibit, Reno, NV, Paper no. AIAA-2007-317*.

[13] Walters, R. W., 2003. "Towards stochastic fluid mechanics via polynomial chaos". *41$^{\text{st}}$ AIAA Aerospace Sciences Meeting and Exhibit, Reno, NV, Paper no. AIAA-2003-0413*.

[14] Hosder, S., Walters, R. W., and Perez, R., 2006. "A non-intrusive polynomial chaos method for uncertainty propagation in CFD simulations". 44$^{\text{th}}$ *AIAA Aerospace Sciences Meeting and Exhibit, Reno, NV, Paper no. AIAA-2006-891*.

[15] Hosder, S., Walters, R. W., and Balch, M., 2008. "Efficient uncertainty quantification applied to the aeroelastic analysis of a transonic wing". 46$^{\text{th}}$ *AIAA Aerospace Sciences Meeting and Exhibit, Reno, NV, Paper no. AIAA-2008-729*.

[16] Reagan, M. T., Najm, H. N., Ghanem, R. G., and Knio, O. M., 2003. "Uncertainty quantification in reacting-flow simulations through non-intrusive spectral projection". *Combustion and Flame,* ***132***, pp. 545–555.

[17] Pettit, C. L., and Beran, P. S., 2006. "Spectral and multiresolution Wiener expansions of oscillatory stochastic process". *Journal of Sound and Vibrtion,* ***294***, pp. 752–779.

[18] Pettit, C. L., and Beran, P. S., 2004. "Polynomial chaos expansion applied to airfoil limit cycle oscillations". *45$^{\text{th}}$ AIAA/ASME/ASCE/AHS/ASC Structures, Structural Dynamics & Materials Conference, California, Paper no. AIAA 2004-1691*.

[19] Fung, Y. C., 1955. *An Introduction to the Theory of Aeroelasticity*. John Wiley & Sons, Inc., New York.

[20] Lee, B., Jiang, L., and Wong, Y., 1998. "Flutter of an airfoil with cubic nonlinearity restoring force". *AIAA Journal,* ***1725***, pp. 237–257.

[21] Wiener, N., 1938. "The homogeneous chaos". *American Journal of Mathematics,* ***60***, pp. 897–936.

[22] Wiener, N., 1958. *Nonlinear Problems in Random Theory*. MIT Technology Press and John Wiley and Sons, New York.

[23] Cameron, R. H., and Martin, W. T., 1947. "The orthogonal development of nonlinear functionals in series of Fourier-Hermite functionals". *Annals of Mathematics,* ***48***, pp. 385–392.

[24] Xiu, D., and Karniadakis, G. E., 2003. "Modelling uncertainty in flow simulations via generalized polynomial chaos". *Journal of Computational Physics,* ***187***, pp. 137–167.

[25] Le Maître, O. P., Knio, O. M., Najm, H. N., and Ghanem, R. G., 2001. "A stochastic projection method for fluid flow: 1.basic formulaton". *Journal of Computational Physics,* ***173(2)***, pp. 481–511.

[26] Witteveen, J. A. S., Sarkar, S., and Bijl, H., 2007. "Modeling physical uncertainites in dynamical stall induced fluid structre interaction of turbine blades using arbitory polynomil chaos". *Computers and Structures,* ***85***, pp. 866–878.

[27] Millman, D., King, P., and Beran, P., 2005. "Airfoil pitch-and-plunge bifurcation behavior with Fourier chaos expansion". *Journal of Aircraft,* ***42***, pp. 376–384.

[28] Millman, D. R., King, P. I., and Beran, P. S., 2003. "A stochastic approach for predicting bifurcation of a pitch and plung airfoil". *21$^{\text{st}}$ AIAA Applied Aerodynamics Conference, Orlando, FL, Paper no. AIAA-2003-3515*.

[29] Millman, D. R., 2004. "Quantifying initial conditions and parametric uncertainties in a nonlinear aeroelastic system with an efficient stochastic algorithm". PhD Thesis, Airforce Institute of Technology, Wright-Patterson Airforce Base, Ohio, September.

[30] Evans, M., and Swartz, T., 2000. *Approximating Integrals via Monte Carlo and Deterministic Methods*. Oxford University Press, Oxford.

[31] Witteveen, J. A. S., and Bijl, H., 2008. "An alternative unsteady adaptive stochastic finite elements formulationbased on interpolation at constant phase". *Comput. Methods Appl. Mech. Engrg.,* ***198***, pp. 578–591.

[32] Witteveen, J. A. S., and Bijl, H., 2009. "Effect of randomness on multi frequency aeroelastic response resolved by unsteady adaptive stochastic finite elements". *Journal of Computational Physics,* ***228***, pp. 7025–7045.

[33] Witteveen, J. A. S., and Bijl, H., 2009. "Higher period stochastic bifurcation of nonlinear airfoil fluid-structure interaction". *Mathematical Problems in Engineering,* ***394387***.